TDO2 modulates liver cancer cell migration and invasion via the Wnt5a pathway

HUI LIU[1*], YUAN XIANG[1,2*], QI-BEI ZONG[1*], ZHOU-TONG DAI[1], HAO WU[3], HUI-MIN ZHANG[1], YOU HUANG[1], CHAO SHEN[1], JUN WANG[1], ZHONG-XIN LU[2], SREENIVASAN PONNAMBALAM[4], KUN CHEN[5], YUAN WU[6], TONG-CUN ZHANG[1,7] and XING-HUA LIAO[1]

[1]Institute of Biology and Medicine, College of Life and Health Sciences, Wuhan University of Science and Technology, Wuhan, Hubei 430081; [2]Department of Medical Laboratory, Central Hospital of Wuhan, Tongji Medical College, Huazhong University of Science and Technology, Wuhan, Hubei 430014; [3]Department of Pathology, Renmin Hospital of Wuhan University, Wuhan, Hubei 430060, P.R. China; [4]School of Molecular and Cellular Biology, University of Leeds, Leeds LS2 9JT, UK; [5]School of Medicine, Liaocheng University, Liaocheng, Shandong 252000; [6]Hubei Cancer Hospital, Tongji Medical College, Huazhong University of Science and Technology, Wuhan, Hubei 430079; [7]Key Laboratory of Industrial Fermentation Microbiology, Ministry of Education and Tianjin, College of Biotechnology, Tianjin University of Science and Technology, Tianjin 300457, P.R. China

Received November 18, 2021; Accepted March 21, 2022

DOI: 10.3892/ijo.2022.5362

Abstract. Liver cancer is a malignant cancer phenotype for which there currently remains a lack of reliable biomarkers and therapeutic targets for disease management. Tryptophan 2,3-dioxygenase (TDO2), a heme-containing polyoxygenase enzyme, is primarily expressed in cells of the liver and nervous systems. In the present study, through the combination of cancer bioinformatics and analysis of clinical patient samples, it was shown that TDO2 expression in liver cancer tissue samples was significantly higher than that in normal tissues, and liver cancer patients with high TDO2 expression had a poor prognosis. Mechanistic studies on liver cancer cells showed that TDO2 promoted cancer cell migration and invasion via signal transduction through the Wnt5a pathway. Such regulation impacted the expression of cancer-associated biomarkers, such as matrix metalloprotease 7 (MMP7) and the cell adhesion receptor CD44. Treatment with a calcium channel blocker (azelnidipine) reduced TDO2 levels and inhibited liver cancer cell migration and invasion. A mouse xenograft cancer model showed that TDO2 promoted tumorigenesis. Furthermore, azelnidipine treatment to downregulate TDO2 also decreased liver cancer development in this mouse cancer model. TDO2 is thus not only a useful liver cancer biomarker but a potential drug target for management of liver cancer.

Correspondence to: Professor Xing-Hua Liao or Professor Tong-Cun Zhang, Institute of Biology and Medicine, College of Life and Health Sciences, Wuhan University of Science and Technology, 947 Heping Avenue, Qingshan District, Wuhan, Hubei 430081, P.R. China
E-mail: xinghualiao@wust.edu.cn
E-mail: zhangtongcun@wust.edu.cn

*Contributed equally

Abbreviations: IOD, integrated optical density; UTR, untranslated region; H&E, hematoxylin and eosin; TDO2, tryptophan 2,3-dioxygenase

Key words: liver cancer, TDO2, microRNA-140-5p, Wnt5a signaling pathway, tumorigenesis, azelnidipine

Introduction

Liver cancer is a frequently occurring malignant cancer that results in more than 700,000 deaths annually worldwide (1,2). Although there are an increasing number of diagnostics methods and therapeutic regimens under development, the prognosis of patients with liver cancer remains poor, and one reason for this poor prognosis is the efficient ability of liver cancer tumors to undergo metastasis leading to the development of secondary tumors in several different organs, ultimately resulting in mortality (3,4). Thus, there is a pressing need to identify novel mechanisms that regulate liver cancer initiation, development and progression to identify new therapeutic targets for management of this disease.

The Wnt signal transduction pathway plays a key biological role in embryonic development, cell fate, and tumorigenesis (5-7). There is a close association between the Wnt signaling pathway and the different factors that regulate early epithelial-mesenchymal transition (EMT) events during tumor metastasis, including cell adhesion markers (CDH1, N-CDH2 and CD44), transcription factors (Snail and Slug) and matrix metalloproteases (MMPs) (8-13). The Wnt signal transduction pathway is commonly divided into β-catenin-dependent (canonical) and β-catenin-independent (non-canonical) signaling arms, which regulate different

biochemical events (5,14). The Wnt signaling pathway has been frequently implicated in liver cancer metastasis and disease development (15-17).

Tryptophan 2,3-dioxygenase (TDO2) is an oxidoreductase, and one of the rate-limiting enzymes involved in the conversion of L-tryptophan to L-kyneurinine, which is the first step in pathway(s) leading to the provision of key biochemical compounds including NAD^+, picolinic acid and glutaryl-CoA. The kyneurinine pathway is primarily expressed in liver and cells of the nervous system, such as neurons (18,19). TDO2 has a key function in not only regulating the catabolic breakdown of tryptophan, but also functions to maintain steady-state homeostasis of cellular tryptophan levels. Upregulation of TDO2 can increase the breakdown of tryptophan and result in the accumulation of kynurenine, thereby inactivating or inhibiting immune cells within the tumor microenvironment, especially T cells. Such biochemical changes can cause tumor cells to evade immune surveillance, allowing tumors to grow and spread rapidly (20,21). Recent studies have found that TDO2 is also highly expressed in tumor cells, such as malignant glioma, liver cancer, malignant melanoma and bladder cancer (22-25). Such findings highlight an association between TDO2 levels with tumor initiation and disease progression; furthermore, TDO2 is implicated in a functional role in the host immune response to tumors.

The aim of the present study was to investigate the functional association between TDO2 and liver cancer, and provide a mechanistic explanation. The results showed that the upregulation of TDO2 expression in liver cancer cells was dependent on a specific microRNA. Increased TDO2 levels impacted signaling via the Wnt5a pathway, leading to increased expression of secreted cancer biomarkers, such as CD44 and MMP7, which was associated with increased liver cancer cell migration and invasion. Furthermore, there was a strong association between TDO2 expression and liver cancer development *in vivo* using a mouse xenograft model of liver cancer.

Materials and methods

Cell culture. Normal liver cells THLE-3 (cat. no. CRL-11233) and hepatocellular carcinoma HepG2 cells (cat. no. HB-8065) were obtained from the American Type Culture Collection. Hepatocellular carcinoma cells Huh7 (cat. no. SCSP-526) were obtained from the Cell Bank of the Chinese Academy of Sciences. All cells were grown in DMEM (Hyclone, Cytiva) supplemented with 10% FBS (Biological Industries) in a humidified incubator (5% CO_2, 37˚C). Liver cancer cells were treated with pan-PKC inhibitor GÖ 6983 (cat. no. HY-13689; MedChemExpress, Inc.) MEK inhibitor U026 (cat. no. HY-12031A; MedChemExpress, Inc.) or calcium channel blocker azelnidipine (cat. no. HY-B0023; MedChemExpress, Inc.) at the indicated concentrations for 0, 24 or 48 h, before being subjected to further analyses, as detailed below. To identify drugs that can reduce TDO2 expression, a library of 1,000 US FDA-approved drugs were screened (Targetmol Co., Ltd.). Briefly, the cells were inoculated in a 6-well plate and then treated with different drugs at a concentration of 25 μM. After 24 h, the cells were collected for protein extraction and validation. All cell lines were free of mycoplasma and were authenticated by genetic profiling using polymorphic short tandem repeat loci.

Collection of clinical samples and analysis. A total of 83 normal (control) liver tissue samples (age range, 38-68 years; mean age, 52; 40 male and 43 female patients) and 98 liver cancer tissue samples (age range, 40-60 years; mean age, 51; 51 male and 47 female patients) were collected from patients who underwent liver biopsy at the Cancer Hospital of Hubei (Wuhan, China). The normal liver samples and the cancer samples were derived from different individuals. All samples were collected from January 2018 to June 2020. All patients provided written informed consent. The present study was approved by the Scientific Ethics Committee of the Cancer Hospital of Hubei (HZ20201018) (Wuhan, China) and the Scientific Ethics Committee of Wuhan University of Science and Technology (WUST200913) (Wuhan, China). The clinical samples were fixed with formalin for immunohistochemical analysis before rapidly freezing in liquid nitrogen for RNA and protein analysis.

Animal studies. For the mouse xenograft studies, 36 4-week-old male BALB/c nude mice (weight, 10-15 g) were purchased from SLAC Laboratory Animal Co. Ltd., and randomly assigned to different groups (n=3 per group), and maintained under pathogen-free conditions. A total of $1x10^6$ HepG2 or Huh7 stable cells were subcutaneously injected into the lower right flank of the nude mice. Measurement of tumor volume, calculated using the formula: $V=L \times W^2 \times 0.5236$ (L=long axis, W=short axis). The tumor weight of the each mouse was not allowed to exceed 10% of the body weight, and the average tumor diameter did not exceed 20 mm. In case of ulceration, infection or necrosis, the experiment was stopped immediately, and the animals were euthanized. All mice were euthanized 4 weeks later, the tumors were excised carefully, and the final tumor weight measured. Mice were euthanized by a peritoneal injection of 200 mg/kg sodium pentobarbital. When the mice stopped breathing and beating for 1 min and the pupils were dilated, the euthanasia was considered complete.

To induce hepatocarcinogenesis, 21 male C57BL/6 mice (2-weeks of age; body weight, 5 g) were intraperitoneally injected with 20 μg/g body weight diethylnitrosamine (DEN; Sigma-Aldrich; Merck KGaA). To increase the expression of TDO2 in liver tissues, from the second week onwards, 100 μl adenovirus solution containing $1x10^9$ adenoviruses were introduced into the mouse peritoneum, once a week for 3 weeks. When the growth of the tumor caused pain to the animal, or the animal lost more than 20% of the body weight of the normal animal, or ulcers, infection, or necrosis appeared, the experiment was stopped immediately and the animal was euthanized. All mice were euthanized after 12 months, and the liver was dissected for the subsequent experiments. Mice were euthanized by a peritoneal injection of 200 mg/kg sodium pentobarbital. When the mice stopped breathing and beating for 1 min and the pupils were dilated, the euthanasia was considered complete. All mice were housed at 23-25˚C, with 50-60% humidity, 12-h light/dark cycle, with food and water *ad libitum*. All experiments on mice were performed under the guidance of the Animal Ethics Committee of Wuhan University of Science and Technology (WS267891).

Molecular biology. The human TDO2 overexpression plasmid pTDO2 was obtained from Addgene. Small interfering (si)RNAs targeting TDO2, Wnt5a, CD44 and MMP7 were obtained from Shanghai GenePharma Co., Ltd. microRNA (miRNA/miR) mimics and the miR-140-5p inhibitor were chemically synthesized by Guangzhou Ribobio Co., Ltd. The siRNA sequences were: siTDO2, 5'-CGUUAAUCGCGUAUAAUACGCGUATT-3'; siCD44, 5'-CUCCCAGUAUGACACAUAUTT-3'; siMMP7, 5'-CUGCUGACAUCAUGAUUGGTT-3'; siWnt5a, 5'-GAAACUGUGCCACUUGUAUTT-3'; siNC 5'-AAUUCUCCGAACGUGUCACGUTT-3'; miR-140-5p mimic, 5'-CAGUGGUUUUACCCUAUGGUAG-3'; miR-140-5p inhibitor, 5'-CUACCAUAGGGUAAAACCACUG-3' and the corresponding negative control, 5'-CAGUACUUUUGUGUAGUACAA-3'. These reagents were used according to standard molecular biology protocols or the manufacturer's instructions.

For total RNA extraction, 1 ml TRIzol® reagent (Invitrogen; Thermo Fisher Scientific, Inc.) was first added to the collected cells for lysis. Chloroform was then added to the lysate to stratify it, the supernatant was taken and a new centrifuge tube was added, and isopropyl alcohol was added to precipitate the RNA. Next, 1 μg RNA was reverse-transcribed into cDNA using an MLV-reverse transcriptase kit (Invitrogen; Thermo Fisher Scientific, Inc.). Reverse transcription-quantitative PCR was performed using SYBR® Premix Ex Taq (Takara Bio, Inc.). The primer sequences were as follows: human *TDO2* forward, 5'-TCCTCAGGCTATCACTACCTGC-3' and reverse, 5'-ATCTTCGGTATCCAGTGTCGG-3'; human *GAPDH* forward, 5'-ATGACATCAAGAAGGTGGTG-3' and reverse 5'-CATACCAGGAAATGAGCTTG-3'. The thermocycling conditions were: 95˚C for 30 sec; followed by 30 cycles of 95˚C for 5 sec, 50˚C for 30 sec and 72˚C for 30 sec. The results were normalized to GAPDH using the $2^{-\Delta\Delta Cq}$ method (26).

Lipofectamine® 2000 (Invitrogen; Thermo Fisher Scientific, Inc.) was used for transfection of all cells. according to the manufacturer's instructions. To generate stable cell lines overexpressing TDO2, HepG2 and Huh7 cells were transduced with a lentivirus construct containing either the TDO2 cDNA or without any insert in the expression cassette; clones were selected using 100 μg/ml G418. TDO2-expressing clonal lines were assessed using RT-qPCR.

Western blotting. For the separation of cytoplasmic and nuclear proteins, a nucleoprotein and cytoplasmic protein extraction kit was used (cat. no. KGP150; KeyGEN BioTECH, Inc.). Briefly, the centrifuged cells were added to the cell membrane lysate and lysed on ice for 10 min to obtain cytoplasmic proteins after centrifugation. Nuclear lysate was added to the remaining precipitate and lysed on ice for 10 min. After centrifugation, the supernatant obtained contained the nuclear proteins. GAPDH was used as a control protein in the cytoplasm and LaminB1 was used as a control protein in the nucleus. For total protein extraction, the cells were lysed with RIPA lysis buffer (Beyotime Institute of Biotechnology) followed by a BCA protein assay, and 30 μg total protein was loaded per lane on an SDS-gel and resolved using 10% SDS-PAGE. Subsequent transfer and blotting were performed using standard protocols. The primary antibodies used were as follows (1:1,000 dilution): anti-TDO2 (cat. no. 15880-1-AP; ProteinTech Group, Inc.), anti-Wnt5a (cat. no. ab179824; Abcam), anti-P-PKC (cat. no. #2060; Cell Signaling Technology, Inc.), anti-P-ERK (cat. no. 28733-1-AP; ProteinTech Group, Inc.), anti-CD44 (cat. no. 15675-1-AP; ProteinTech Group, Inc.), anti-MMP7 (cat. no. 10374-2-AP; ProteinTech Group, Inc.) and anti-GAPDH (cat. no. #5174; Cell Signaling Technology, Inc.). The PVDF membrane was incubated with the primary antibody at 4˚C overnight. After being washed three times with TBST Buffer, the PVDF membrane was then incubated with the corresponding secondary antibody (1:10,000 dilution; cat. no. SA00001-2; ProteinTech Group, Inc.) for 1 h at the shaker. Finally, the blotted proteins were observed using BeyoECL Plus (cat. no. P0018S; Beyotime, Inc.), and the quantification of the blots was analyzed using ImageJ version 1.8.0 (National Institutes of Health).

Cell monolayer wound closure assay. Liver cancer cells ($4x10^5$) were incubated in a 6-well plate; 12 h later the confluent cell monolayer was wounded across the well diameter using a 200-μl sterile pipette tip. The wounded cell monolayer was then washed twice with fresh cell culture medium. Digital images of the wounded cell monolayer were collected at 0 and 48 h using an inverted microscope. The wound surface area was assessed using ImageJ software (version 1.8.0), and the wound healing activity of the colon cancer cells was determined by the quantification of wound healing progression. Wound healing activity=1-(wound surface area at the indicated time-point/wound surface area at baseline). Serum-free medium was used during the experiment.

Cell migration and invasion assays. Transwell assays were performed using Corning permeable cell culture chambers. Briefly, $1x10^5$ cells were mixed into 100 μl of serum-free medium, then the cell suspension was seeded into the upper chamber, while the lower chamber contained 600 μl media supplemented with 10% FBS. After 24 h of incubation, the Transwell inserts were removed, and cells were gently wiped away from the upper chamber using cotton swabs, and next the Transwell filter (containing cells on the bottom) was fixed in 100% methanol for 10 min, rinsed in PBS and stained with 0.05% (w/v) crystal violet for 30 min. After washing, the filters were removed and mounted under coverslips on slides. Using bright field microscopy and digital imaging, five areas were randomly selected in each field of view at x100 magnification, and imaged and analyzed.

Immunohistochemistry. The tissues were immersed in 4% (w/v) paraformaldehyde and fixed for 24 h, and then the tissues were dehydrated, embedded in paraffin and cut into 5-μm sections. Hematoxylin and eosin staining was performed according to standard protocols. Paraffin sections were deparaffinized in xylene and then rehydrated using a concentration gradient alcohol. The processed tissue sections were subjected to heat-induced antigen recovery by incubation in a citrate buffer at 100˚C for 10 min. The tissue sections were incubated with the antibody in blocking buffer: anti-TDO2 antibody (cat. no. 15880-1-AP, ProteinTech Group, Inc.), anti-Wnt5a antibody (cat. no. ab179824, Abcam), anti-MMP7 (cat. no. 10374-2-AP, ProteinTech Group, Inc.) or anti-CD44 antibody (cat. no. 15675-1-AP, ProteinTech Group, Inc.),

overnight at 4˚C. After extensive washing, the sections were incubated with species-specific HRP-conjugated secondary antibody in blocking buffer (Sangon Biotech, Co., Ltd.) at 25˚C for 45 min. The sections were washed extensively, incubated with DAB chromogenic reagent, counterstained with hematoxylin, rinsed and mounted on microscope glass slides using neutral resin.

Bioinformatics analysis. miRNAs binding to target genes were analyzed by DIANA (http://diana.imis.athena-innovation.gr/DianaTools/index.php?r=lncBase/index), MIRDB (http://mirdb.org/), TargetScan (http://www.targetscan.org/vert_71/) and mirDIP (http://ophid.utoronto.ca/mirDIP/index_confirm.jsp) databases.

Statistical analysis. All experimental data are presented as the mean ± SEM of at least 3 independent experiments. Statistical analysis was performed using GraphPad Prism 8.0.2 software (GraphPad Software, Inc.). Data were analyzed using an unpaired Student's t-test when comparing two groups. Comparisons between multiple groups were performed using a one-way ANOVA followed by a Tukey's post hoc test. $P<0.05$ was considered to indicate a statistically significant difference.

Results

Elevation of TDO2 in liver cancer disease. To investigate whether TDO2 expression is elevated in clinical samples from patients with liver cancer, TDO2 expression levels in control and liver cancer clinical specimens were analyzed using immunohistochemistry. Liver cancer samples consistently showed upregulation of TDO2 expression (Fig. 1A and B). Western blot analysis consistently revealed increased TDO2 protein expression in liver cancer compared with control clinical samples (Fig. 1C and D). RT-qPCR data from control and liver cancer clinical samples revealed no significant difference in *TDO2* mRNA levels in liver cancer samples compared with the normal control liver samples (Fig. 1E). These data showed that TDO2 expression is increased in liver cancer disease.

Increased TDO2 expression promotes liver cancer cell migration and invasion. To further explore the biological role of TDO2 in liver cancer, HepG2 and Huh7 cell lines were transduced with a TDO2 expression plasmid (pTDO2) or a control plasmid (empty vector; pcDNA3.1). In TDO2-overexpressing HepG2 and HuH7 cells, a significant increase in liver cancer cell migration and invasion was observed compared with cells transduced with the control plasmid (Fig. S1A and B). A similar picture emerged when RNA interference (RNAi) was used to assess the role of TDO2 expression in liver cancer cell migration and invasion. Compared with the control group (siCon), TDO2 knockdown (siTDO2) significantly reduced the wound closure (Fig. S1C) and migratory and invasive abilities of the cells (Fig. S1D). Increased TDO2 expression thus correlates with increased liver cancer cell migration and invasion.

miR-140-5p targets the TDO2 mRNA 3'-untranslated region (UTR) to inhibit TDO2 expression. Bioinformatics analysis of miRNAs from different databases (TargetScan, miRDB, mirDIP and DIANA) suggest that miR-140-5p is a potential regulator of TDO2 expression in normal vs. liver cancer disease states (Fig. 2A). Using RT-qPCR analysis, miR-140-5p was found to be significantly downregulated in liver cancer cells (HepG2 and Huh7) compared with the control liver cells (THLE-3) (Fig. 2B). Furthermore, RT-qPCR analysis of miR-140-5p in the control and liver cancer specimen showed that miR-140-5p levels were significantly downregulated in the liver cancer samples compared with the controls (Fig. 2C). Analysis of TDO2 vs. miR-140-5p levels showed an inverse correlation in the liver cancer clinical samples (Fig. 2D); that is reduced miR-140-5p levels correlated with increased TDO2 levels in liver cancer disease.

Bioinformatics algorithms (TargetScan, miRDB, mirDIP and DIANA) were used, and they revealed a potential binding site for miR-140-5p in the 3'UTR of the *TDO2* mRNA (Fig. 2E). To test this potential interaction, two reporter vectors consisting of the luciferase-coding sequence followed by the 3'UTR of wild-type TDO2 (WT-TDO2 3'-UTR) or mutant 3'-UTR (Mut-TDO2 3'-UTR) were constructed (Fig. 2E). Transient transfection of these constructs into HepG2 or Huh7 liver cancer cells followed by luciferase assay showed that miR-140-5p decreased luciferase activity when co-expressed alongside WT-TDO2 3'UTR; however, miR-140-5p had little to no effect on luciferase activity with Mut-TDO2 3'UTR (Fig. 2F). As these data suggested that miR-140-5p could directly bind to the TDO2 3'UTR, miR-140-5p mimics or mimic NC were transfected into HepG2 and Huh7 cells. The results showed that miR-140-5p mimics decreased both HepG2 and Huh7 monolayer wound closure, cell migration and invasion (Fig. S2A and B). Consistent with this, an inhibitor of miR-140-5p showed the reverse effect; an increase in HepG2 and Huh7 monolayer wound closure, cell migration and invasion was observed (Fig. S2C and D). These data suggest that miR-140-5p inhibits TDO2 expression by directly binding to the 3'UTR of *TDO2* mRNA in HepG2 and Huh7 cell lines.

Elevated levels of TDO2 are associated with increased CD44 and MMP7 expression. To investigate the mechanism underlying the effects of TDO2-mediated liver cancer cell migration and invasion, expression of EMT biomarkers associated with liver cancer development and progression was assessed. Overexpression of TDO2 resulted in a significant increase in N-cadherin and fibronectin levels; conversely, TDO2 overexpression resulted in a decrease in the expression of the tumor suppressor, E-cadherin (Fig. S3A). Next, the expression of other biomarkers related to cancer metastasis were examined. Western blotting showed that overexpression of TDO2 significantly increased CD44 and MMP7 levels (Fig. 3A). However, expression of other cancer biomarkers, such as MMP9, MMP2 and c-Met were not affected (Fig. 3A).

Next, whether CD44 and MMP7 contribute to liver cancer cell properties, such as wound closure, cell migration and invasion was assessed (Figs. S4 and S5). CD44 expression was knocked down using siRNA (siCD44) in both HepG2 and Huh7 cell lines overexpressing TDO2 (Fig. S4A). Consistently, the enhancement of monolayer wound closure, cell migration and invasion caused by TDO2 overexpression was significantly inhibited following siCD44 transfection (Fig. S4B and C). Next, MMP7 expression was knocked down using siRNA (siMMP7) in both HepG2 and Huh7 cells overexpressing

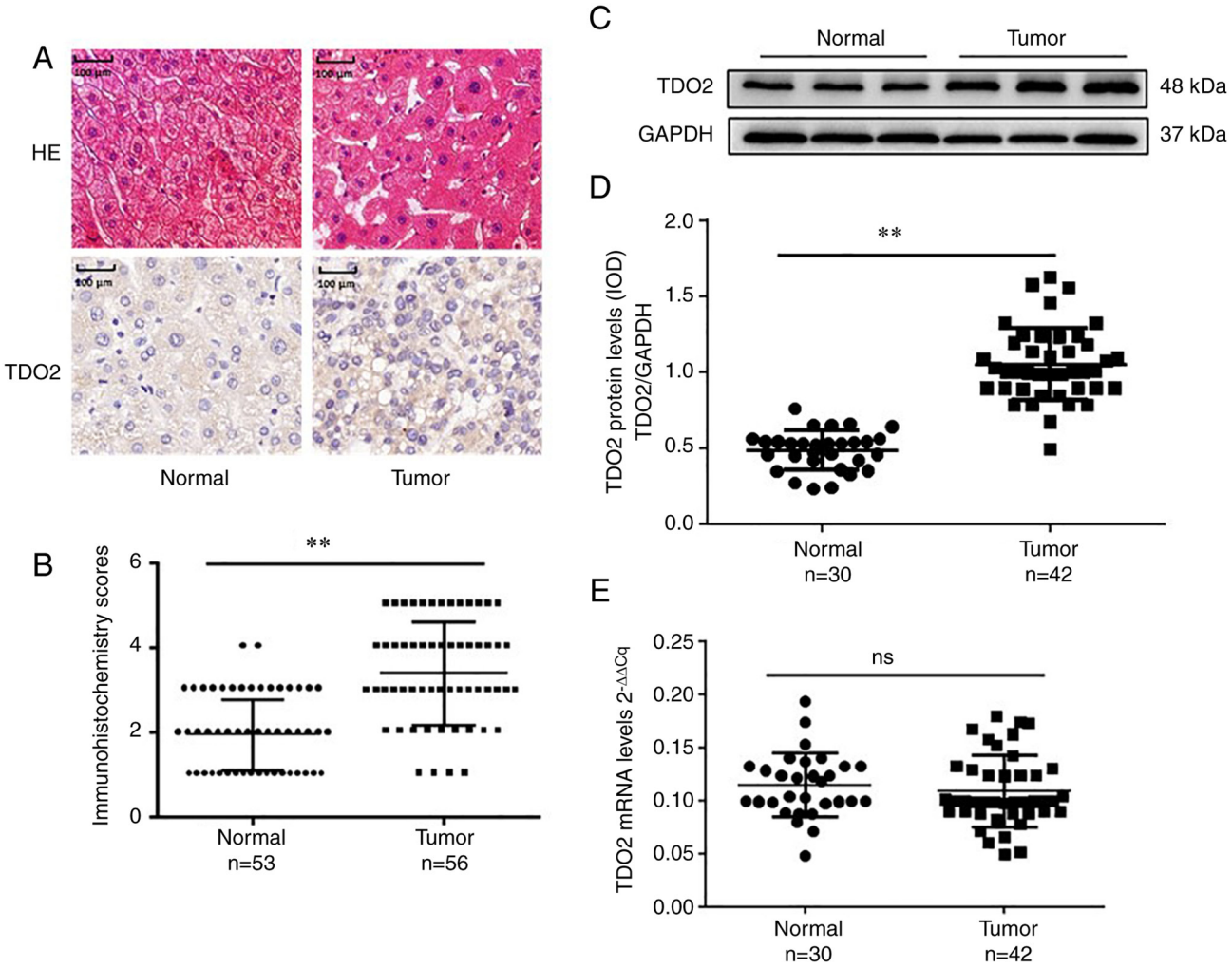

Figure 1. TDO2 expression is increased in liver cancer. (A) TDO2 expression in control and liver cancer clinical specimens using immunohistochemistry. Representative immunohistochemistry images are shown. (B) Semi-quantitative analysis of TDO2 protein expression in the control (n=53) and liver cancer (n=56) samples from the immunohistochemistry datasets. (C) Western blot analysis of TDO2 and GAPDH protein levels; 3 representative samples of control and liver cancer samples are shown. (D) TDO2 and GAPDH protein levels were determined via densitometry using ImageJ and are presented as the IOD (E) Quantification of *TDO2* mRNA levels using reverse transcription-quantitative PCR. Data are presented as the mean ± SEM. **P<0.01; ns, not significant; TDO2, tryptophan 2,3-dioxygenase; IOD, integrated optical density; H&E, hematoxylin and eosin.

TDO2 (Fig. S5A). In HepG2 or Huh7 cells, downregulation of the MMP7 gene also offsets the enhancement of wound healing, cell migration and invasion caused by TDO2 overexpression (Fig. S5B and C). These data suggest that the elevated expression of CD44 and MMP7 biomarkers provide important supporting roles in liver cancer cell migration and invasion.

TDO2 activates the Wnt5a signal transduction pathway. CD44 and MMP7 are both downstream target genes of the Wnt/β-catenin signal transduction pathway (11,27,28). This then raised the question as to whether TDO2 affects signaling through the Wnt/β-catenin signaling pathway. Western blotting showed that TDO2 overexpression did not affect components of the Wnt/β-catenin pathway such as β-catenin and c-Myc (Fig. S3B).

Importantly, upon TDO2 overexpression, other components of the Wnt5a signal transduction pathway exhibited changes in both HepG2 and Huh7 cells (Fig. 3B). Overexpression of TDO2 caused a significant increase in Wnt5a levels (Fig. 3B). Furthermore, the levels of phospho-protein kinase C (ζ) (P-PKC) as in the figure were significantly elevated in the TDO2 overexpressing cells (Fig. 3B). In HepG2 and Huh7 cells overexpressing TDO2, phospho-ERK1/2 (P-ERK) levels were elevated (Fig. 3C), indicating activation of the MAPK pathway.

To examine the association between TDO2 and the Wnt5a signal transduction pathway, the effects of Wnt5a knockdown (siwnt5a) in HepG2 and Huh7 cells overexpressing TDO2 were examined (Fig. S6). Interestingly, knockdown of Wnt5a in TDO2-overexpressing HepG2 or Huh7 cells completely blocked the increase in P-PKC, CD44 and MMP7 levels (Fig. S6A). Furthermore, knockdown of Wnt5a consistently caused a decrease in monolayer wound closure, cell migration and invasion in both the control and TDO2-overexpressing HepG2 or Huh7 cells (Fig. S6B and C).

To examine the association between TDO2 and the Wnt5a signal transduction pathway, the effects of pan-PKC inhibitor GÖ 6983 treatment on HepG2 and Huh7 cells overexpressing TDO2 were determined (Fig. S7). Again, pan-PKC inhibition blocked PKC phosphorylation (P-PKC), and decreased

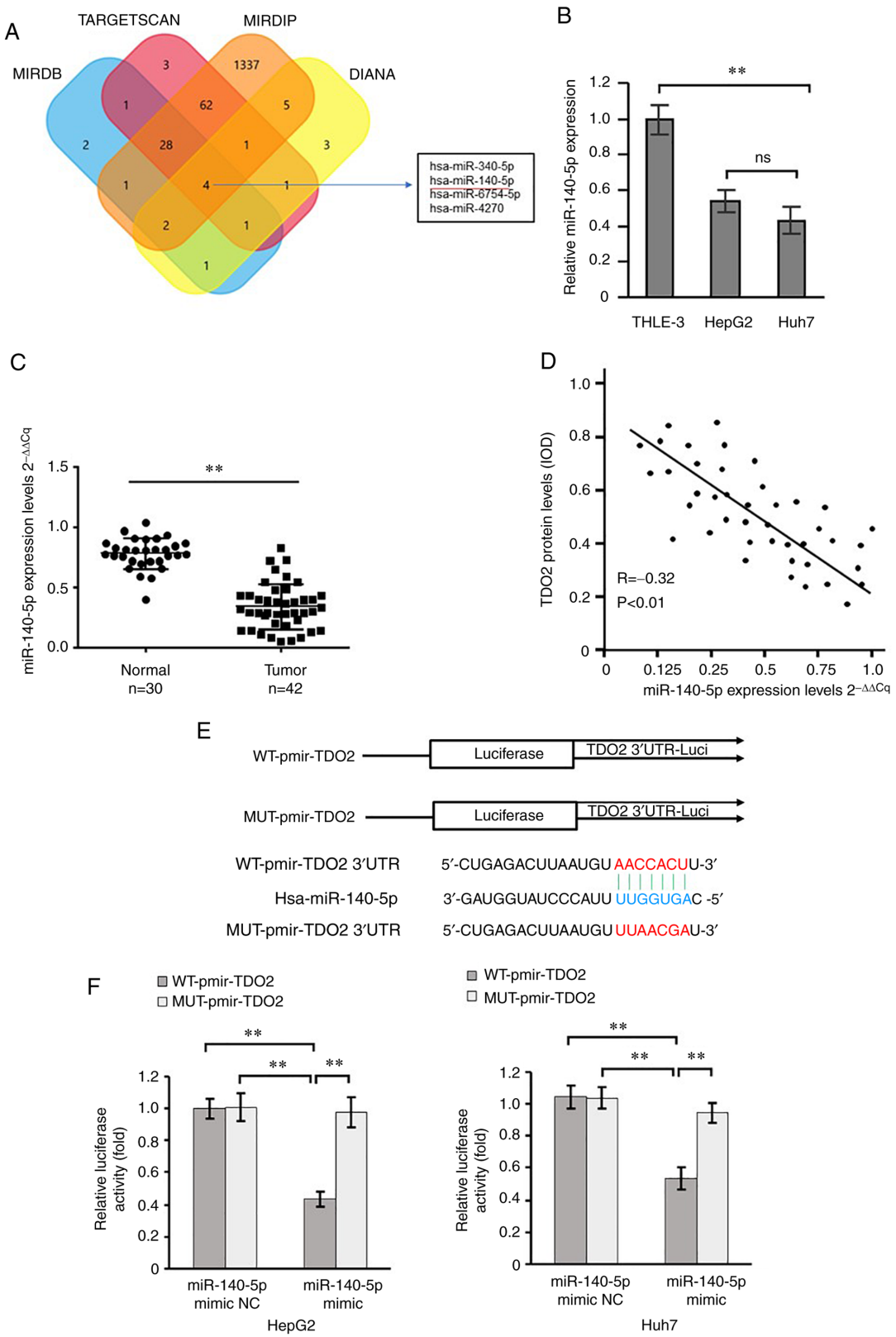

Figure 2. *TDO2* mRNA is a direct target of miR-140-5p. (A) The four-way Venn diagram indicates the numbers of miRNAs that overlapped in four publicly available bioinformatics algorithms with a TDO2 signature. The four-way Venn diagram was analyzed by DIANA (http://diana.imis.athena-innovation.gr/DianaTools/index.php?r=lncBase/index), MIRDB (http://mirdb.org/), TargetScan (http://www.targetscan.org/vert_71/) and mirDIP (http://ophid.utoronto.ca/mirDIP/index_confirm.jsp) databases. (B) Reverse transcription-quantitative PCR analysis of miR-140-5p levels in control liver (THLE-3) and liver cancer (HepG2 and HuH7) cells. (C) miR-140-5p levels were quantified in 30 normal control liver tissues and 42 liver cancer samples from patients. (D) Correlation between TDO2 protein levels and miR-140-5p levels in 42 liver cancer patient samples that we collected. (E) Schematic showing the synthesis of the WT and MUT *TDO2* mRNA 3'UTR sequences to luciferase reporters. The potential miR-140-5p-binding site in the *TDO2* mRNA 3'UTR is highlighted. It was from TargetScan (http://www.targetscan.org/vert_71/). (F) Luciferase activity measurements in HepG2 and Huh7 cells transfected with luciferase reporter plasmids carrying either WT-pmir-TDO2 or MUT-pmir-TDO2 sequences, and co-expressing either miR-140-5p mimic or miR-140-5p mimic NC. Data are presented as the mean ± SEM. **P<0.01. TDO2, tryptophan 2,3-dioxygenase; miR, microRNA; UTR, untranslated region; NC, negative control; WT, wild-type; MUT, mutant; RIP, RNA immunoprecipitation.

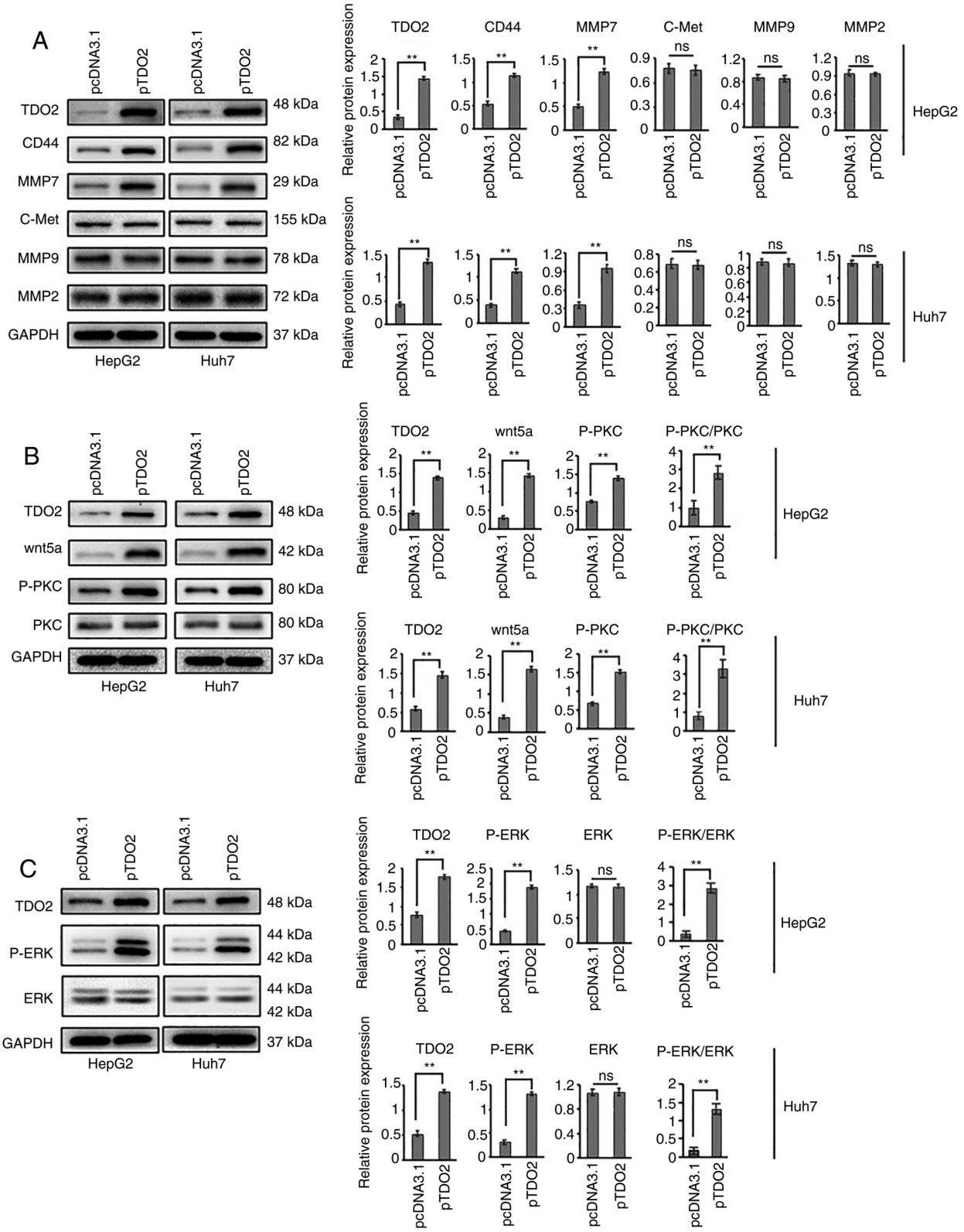

Figure 3. TDO2 activates the Wnt5a pathway to promote the expression of CD44 and MMP7. HepG2 and Huh7 cells were transfected with plasmids pTDO2 or pcDNA3.1. Western blotting of transfected HepG2 (left hand panels) and Huh7 (right hand panels) cell lines expressing either pCDNA3.1 or pTDO2 (A) for markers of cancer cell migration; (B) for components of the Wnt5a signaling pathway, including Wnt5a and phospho-(P)-PKC; and (C) to detect ERK1/2 phosphorylation (P-ERK). Data are presented as the mean ± SEM. **P<0.01; ns, not significant; TDO2, tryptophan 2,3-dioxygenase; MMP, matrix metalloprotease; P-PKC, phospho-protein kinase C.

expression of CD44 and MMP7 (Fig. S7A), consistent with PKC signaling influencing expression of these key secreted cancer biomarkers. Pan-PKC inhibition caused a significant decrease in monolayer wound closure, cell migration and invasion in both control and TDO2-overexpressing HepG2 or Huh7 cells. The use of GÖ 6983 offset the enhancement

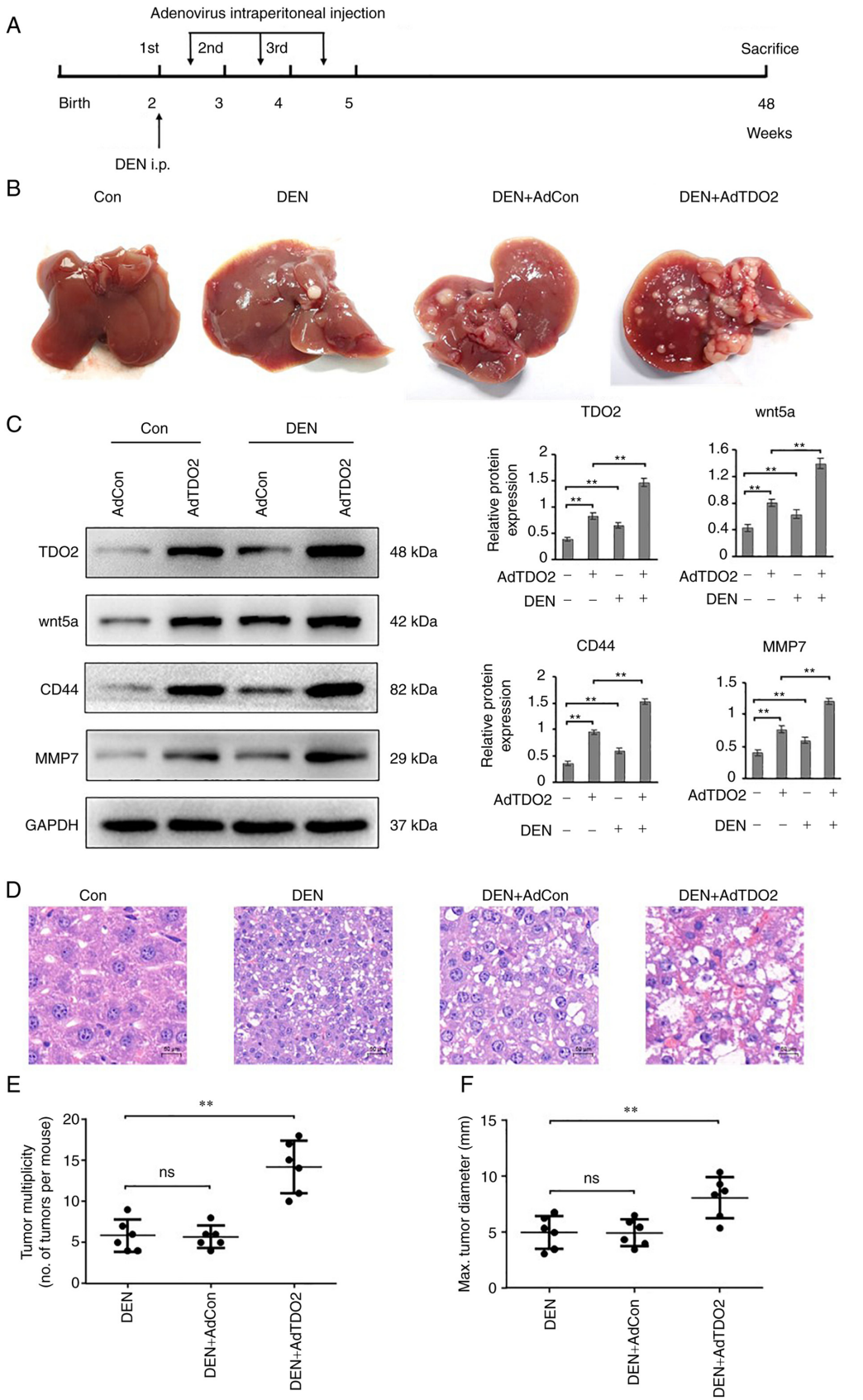

Figure 4. TDO2 accelerates DEN-induced liver tumor progression in C57BL/6 mice. (A) Schematic of the experimental setup: 2-week-old male C57BL/6 mice were injected intraperitoneally (i.p.) with 20 μg/g DEN. To increase TDO2 expression in liver tissues, adenoviruses containing the TDO2 expression cassette was introduced into the mouse peritoneum, once a week for 3 weeks. All mice were euthanized at 12 months of age. Mice that received normal drinking water and were not instilled with adenovirus were used as the control. (B) Representative images of the gross mouse livers. (C) TDO2, Wnt5a, CD44 and MMP7 expression in liver tissues were determined by western blotting. (D) Representative microscopic features of liver cancer in H&E-stained liver sections from mice. (E) Tumor numbers in the mouse liver. (F) Average maximal diameters of the tumors. Scale bar, 50 mm. Data are presented as the mean ± SEM of at least 3 mice per group. **P<0.01; ns, not significant; TDO2, tryptophan 2,3-dioxygenase; DEN, diethylnitrosamine; H&E, hematoxylin and eosin; MMP, matrix metalloprotease.

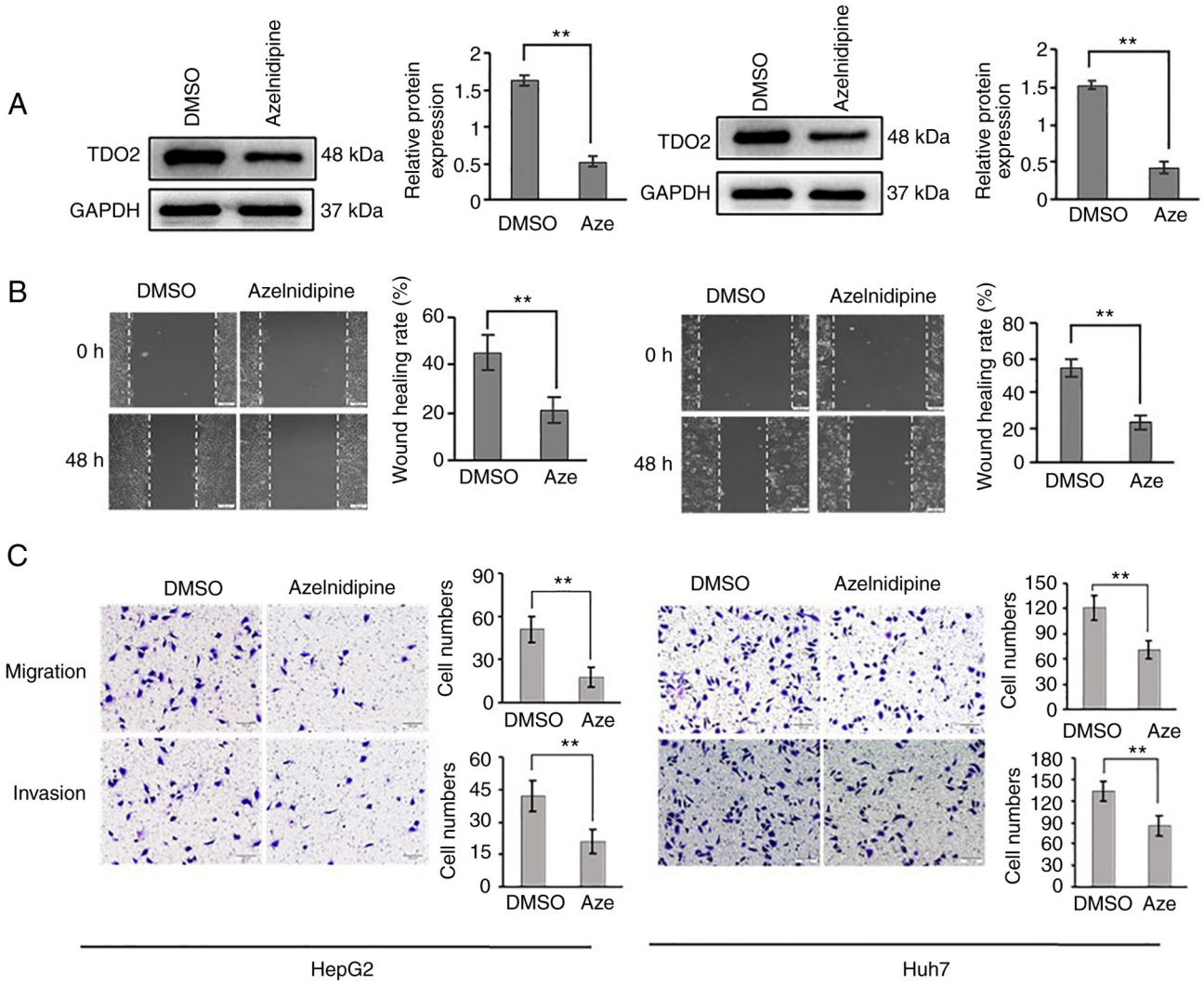

Figure 5. Azelnidipine inhibits TDO2 expression and liver cancer cell migration and invasion. (A) HepG2 and Huh7 cells were treated with 20 μM azelnidipine (Aze) for 24 h before cell lysis and immunoblotting for TDO2 and GAPDH. (B) Wound healing assays with the liver cancer cells were performed using HepG2 and Huh7 cells treated with 20 μM azelnidipine and compared with the control (0 μM). Cells were observed at 0 and 48 h after treatment. (C) Transwell migration and Matrigel invasion assays using HepG2 and Huh7 cells treated with 20 μM azelnidipine for 24 h. Data are presented as the mean ± SEM. **P<0.01. TDO2, tryptophan 2,3-dioxygenase.

of wound healing, cell migration and invasion caused by TDO2 overexpression. (Fig. S7B and C). Another pharmacological inhibitor, U0126, was found to inhibit MEK protein kinase and signaling through the canonical MAPK pathway (Fig. S8). Testing U0126 in this context again revealed a block in the TDO2-induced increase in CD44 and MMP7 levels (Fig. S8A). Furthermore, U0126 also caused a decrease in liver cancer cell migration and invasion in the control and TDO2-overexpressing cells in the liver cancer cells (Fig. S8B and C). These data suggest a close functional link between the TDO2, Wnt5a, PKC and MAPK pathways in controlling HepG2 and Huh7 cell migration and invasion.

TDO2 overexpression promotes tumorigenesis in vivo. In order to study the association between TDO2 expression with liver cancer tumor development and progression *in vivo*, the effect of TDO2 on the prevalence of DEN-induced liver cancer in C57BL/6 mice was assessed. C57BL/6 mice were intraperitoneally injected with 20 μg/g body weight diethylnitrosamine. To increase the expression of TDO2 in liver tissues, from the second week onwards, 100 μl adenovirus solution containing $1x10^9$ adenoviruses were introduced into the mouse peritoneum, once a week for 3 weeks (Fig. 4A). The results showed that TDO2 overexpression in the liver tissues significantly enhanced tumor multiplicity (Fig. 4B). Western blotting showed increased expression of TDO2 was paralleled with increased Wnt5a, CD44 and MMP7 expression (Fig. 4C). H&E staining showed that TDO2 increased the atypia of liver cancer in mice (Fig. 4D). TDO2 overexpression in the liver tissues of liver cancer mouse models not only enhanced the severity of liver cancer, but also markedly enhanced the number of liver tumors (Fig. 4E and F).

A mouse xenograft model was also used to study the association between TDO2 expression with liver cancer development and progression. In these experiments, an immunocompromised nude mouse was used and subcutaneously injected into HepG2 or Huh7 cells stably overexpressing TDO2. Consistently, there was an increase in tumor volume and weight, and TDO2 serum levels in liver cancer cells overexpressing TDO2 compared with the control (Fig. S9A-C).

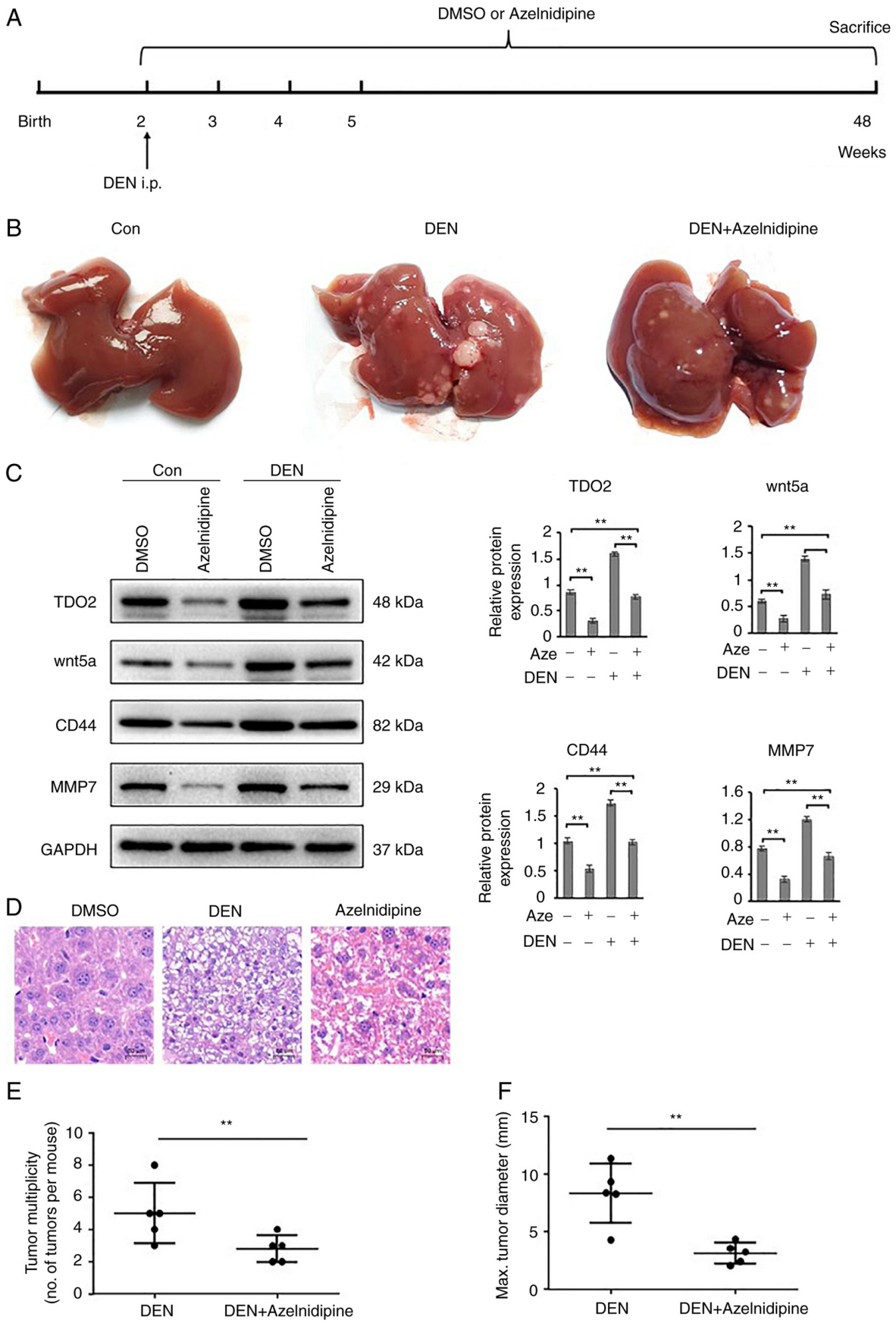

Figure 6. Inhibition of TDO2 expression by azelnidipine prevents tumorigenesis in C57BL/6 mice. (A) Schematic diagram of the experimental setup: 2-week-old male C57BL/6 mice were injected intraperitoneally (i.p.) with 20 μg/g DEN. To reduce TDO2 expression in liver tissues, 28 mg/kg azelnidipine was added to the drinking water. (B) Representative images of the gross mouse liver. (C) TDO2, Wnt5a, CD44 and MMP7 expression in liver tissues were determined by western blotting. (D) Representative microscopic features of liver cancer in the H&E-stained liver sections from mice. (E) Tumor numbers in the mouse liver. (F) Average maximal diameters of tumors. Scale bar, 50 mm. Data are presented as the mean ± SEM of at least 3 mice per group. **P<0.01. H&E, hematoxylin and eosin; TDO2, tryptophan 2,3-dioxygenase; DEN, diethylnitrosamine; MMP, matrix metalloprotease.

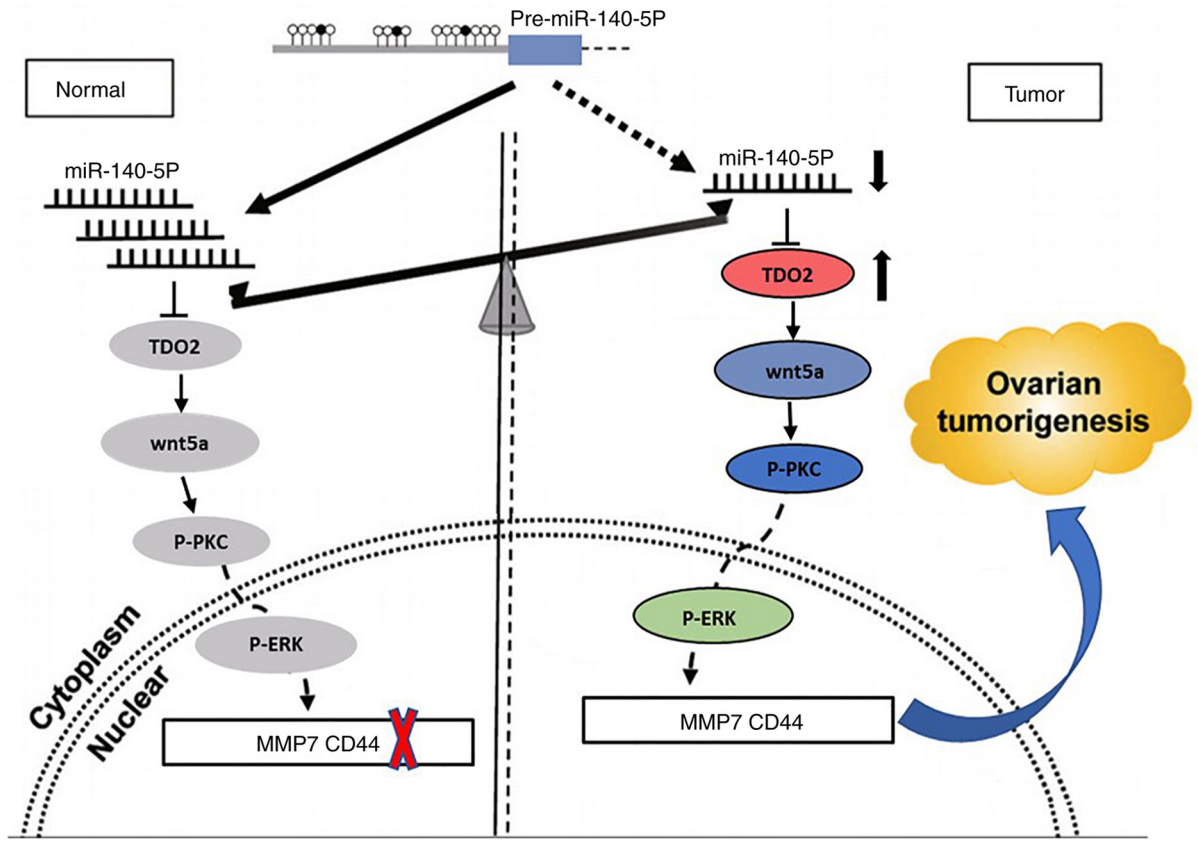

Figure 7. Schematic diagram showing the proposed mechanism by which TDO2 regulates liver cancer tumorigenesis. Under normal non-transformed conditions, miR-140-5p binds to the 3'UTR in the *TDO2* mRNA and downregulates TDO2 protein levels. In liver cancer, there are reduced levels of miR-140-5p, leading to elevated TDO2 expression levels, and thus activation of the Wnt5a signaling pathway, and increased expression of MMP7 and CD44. TDO2, tryptophan 2,3-dioxygenase; MMP, matrix metalloprotease; P-PKC, phospho-protein kinase C; UTR, untranslated region.

Immunohistochemistry analysis of tumor sections showed increased expression of TDO2 was paralleled with increased Wnt5a, CD44 and MMP7 expression (Fig. S9D). These data suggest that TDO2 overexpression promotes liver cancer development and progression *in vivo*.

Reduction of TDO2 expression inhibits the tumorigenesis in liver. To determine a pharmacological route for blocking TDO2 promotion of liver cancer disease, a small molecule drug library was screened. A calcium channel blocker, azelnidipine (Aze), was found to be able to decrease TDO2 levels in the HepG2 and Huh7 cell lines (Fig. 5A). Treatment with azelnidipine caused a decrease in cell migration and invasion (Fig. 5B and C). Overexpression of TDO2 in these liver cancer cells partially overcame the pharmacological effects of azelnidipine (Fig. S10). Notably, TDO2 overexpression re-established the elevation in CD44 and MMP7 levels (Fig. S10A); furthermore, although azelnidipine caused a decrease in cell migration and invasion, there was a consistent increase in these parameters in TDO2-overexpressing cells compared with the controls (Fig. S10B and C).

Administration of azelnidipine to the liver cancer mouse models reduced TDO2 expression in the liver tissues (Fig. 6A-C). Pharmacological reduction of TDO2 expression in the liver cancer mouse model alleviated the severity of liver cancer and liver tumor numbers (Fig. 6D-F). Similar to liver cancer mouse models, azelnidipine reduced tumor volume, weight and serum TDO2 level in the mouse xenograft tumor model (Fig. S11A-D and Fig. S11F-I). Immunohistochemistry analysis of tumor sections showed that azelnidipine reduced the expression of TDO2, Wnt5a, CD44 and MMP7 (Fig. S11E and Fig. S11J).

Discussion

In the present study, it was shown that the expression of tryptophan 2,3-dioxygenase (TDO2) was upregulated in clinical samples of liver cancer compared with a control patient group. By combining bioinformatics analysis and experimental studies, miR-140-5p was determined to mediate an inhibitory effect on TDO2 expression, largely mediated by the binding of miR-140-5p to the 3'UTR of the *TDO2* mRNA. Analysis of miR-140-5p levels in the control and liver cancer samples indicated that lower miR-140-5p levels were correlated with reduced overall survival in patients with liver cancer. There was a clear association between elevated TDO2 levels and activation of the Wnt5a signal transduction pathway: There was increased activation of the PKC (isoform) and the canonical MAPK pathway, resulting in increased expression of matrix metalloprotease 7 (MMP7) and the cell adhesion receptor CD44 cancer biomarkers. These findings showing that TDO2 promotes liver cancer disease progression is supported by other studies, which have also highlighted a role for TDO2 in promoting tumor development and progression in multiple

disease states including skin (18), breast (29) and non-small cell lung cancer (30).

Aberrant miRNA expression frequently leads to abnormal expression of a range of target genes. miR-140-5p is known to suppress tumor growth and metastasis by targeting fibroblast growth factor 9 and transforming growth factor (TGF)β receptor 1 (31). miR-140-5p functions as a tumor suppressor in breast, ovarian and non-small cell lung cancer (32-34). The results of the present study propose a novel role for miR-140-5p in modulating TDO2 expression, and this is a major driver in liver cancer development and progression (Figs. 7 and S12).

How TDO2 enzymatic activity influences cancer development and progression was also assessed. TDO2 encodes a heme-containing enzyme and oxidoreductase that plays a critical role in tryptophan metabolism by catalyzing the first and rate-limiting step of the kynurenine pathway. Previous reports have found that TDO2 plays an important role in the occurrence and development of breast and brain cancer; this enzyme also promotes the activation of AHR and increases the Kyn/TPR ratio in a range of cancers (29,34-37). In the present study, the increased levels of TDO2 activated the Wnt5a signal transduction pathway causing an increase in MMP7 and CD44 expression in liver cancer cells and xenograft tumors. Administration of an miR-140-5p mimic or RNAi-mediated TDO2 knockdown caused a corresponding decrease in CD44 and MMP7 levels. Interestingly, in the liver cancer samples, decreased levels of miR140-5p were correlated with increased TDO2 levels, and reduced overall liver cancer patient survival. These findings provide a strong mechanistic link between the increased TDO2 levels and increased signaling through the Wnt5a pathway in liver cancer; increased expression of CD44 and MMP7 could thus contribute to liver cancer development and progression. Furthermore, increased TDO2 expression also modulates epithelial-mesenchymal transition (EMT) biomarkers such as E-cadherin, N-cadherin and fibronectin suggesting further effects on the EMT phenotype, which is implicated in tumor metastasis.

Azelnidipine is a dihydropyridine calcium channel blocker, and is widely used as a first-line hypertension treatment due to the reliability of its antihypertensive effect. Azelnidipine has diuretic, cardioprotective, renal protective and anti-arteriosclerotic effects (38,39). In the present study, it was found that azelnidipine could be used to inhibit liver cancer cell migration and metastasis by inhibiting TDO2 expression. Although the molecular mechanism by which azelnidipine inhibits TDO2 expression is still unclear, it is unlikely to directly involve cytosolic calcium ion levels. This was based on the result that nifedipine, another dihydropyridine and long-acting calcium antagonist, did not affect TDO2 expression (Fig. S13).

Acknowledgements

We would like to thank Dr Hao Hu and Dr Jizao Yang (The First Affiliated Hospital of Nanjing Medical University, China) for their assistance with the pathology techniques.

Funding

This study was financially supported by the National Natural Science Foundation of China (grant nos. 31501149, 31770815 and 31570764) and Hubei Natural Science Foundation (grant no. 2017CFB537) and the Educational Commission of Hubei (grant no. B2020001), Hubei Province Health and Family Planning Scientific Research Project (grant nos. WJ2021Q051 and WJ2019M255), the Frontier Project of Applied Basic Research in Wuhan (grant no. 2020020601012250) and The Royal Society International Exchanges UK-China Award (grant no. IEC\NSFC\181262).

Availability of data and materials

The datasets used and/or analyzed during the present study are available from the corresponding author on reasonable request.

Authors' contributions

XHL conceived and devised the study. XHL, QBZ, ZTD, HW, SP, KC, YW, HL, ZXL, TCZ and YX designed the experiments and performed the analysis. HL, YX, ZTD, HMZ, YH, CS, KC, YW and JW performed the experiments and analyzed the data. HW, ZXL and TCZ confirm the authenticity of all the raw data. SP and XHL wrote the manuscript. All authors read and approved the final manuscript for publication.

Ethics approval and consent to participate

The study was approved by the Scientific Ethics Committee of the Cancer Hospital of Hubei (HZ20201018) and the Scientific Ethics Committee of Wuhan University of Science and Technology (WUST200913) (Wuhan, China) and was conducted in accordance with the Declaration of Helsinki. Written informed consents were obtained from all participants. The animal study was reviewed and approved by the Animal Ethics Committee of Wuhan University of Science and Technology (WS267891) (Wuhan, China).

Patient consent for publication

Not applicable.

Competing interests

The authors declare that they have no competing interests.

References

1. Li LY, Yang JF, Rong F, Luo ZP, Hu S, Fang H, Wu Y, Yao R, Kong WH, Feng XW, *et al*: ZEB1 serves an oncogenic role in the tumourigenesis of HCC by promoting cell proliferation, migration, and inhibiting apoptosis via Wnt/β-catenin signaling pathway. Acta Pharmacol Sin 42: 1676-1689, 2021.
2. Ichikawa T, Sano K and Morisaka H: Diagnosis of pathologically early hcc with eob-mri: Experiences and current consensus. Liver Cancer 3: 97-107, 2014.
3. Gentile D, Donadon M, Lleo A, Aghemo A, Roncalli M, di Tommaso L and Torzilli G: Surgical treatment of hepatocholangiocarcinoma: A systematic review. Liver Cancer 9: 15-27, 2020.
4. Xie KL, Zhang YG, Liu J, Zeng Y and Wu H: MicroRNAs associated with HBV infection and HBV-related HCC. Theranostics 4: 1176-1192, 2014.
5. Hall CL, Kang S, MacDougald OA and Keller ET: Role of Wnts in prostate cancer bone metastases. J Cell Biochem 97: 661-672, 2006.

6. Hu HH, Cao G, Wu XQ, Vaziri ND and Zhao YY: Wnt signaling pathway in aging-related tissue fibrosis and therapies. Ageing Res Rev 60: 101063, 2020.
7. Caspi M, Wittenstein A, Kazelnik M, Shor-Nareznoy Y and Rosin-Arbesfeld R: Therapeutic targeting of the oncogenic Wnt signaling pathway for treating colorectal cancer and other colonic disorders. Adv Drug Deliv Rev 169: 118-136, 2021.
8. Zhi X, Lin L, Yang S, Bhuvaneshwar K, Wang H, Gusev Y, Lee MH, Kallakury B, Shivapurkar N, Cahn K, *et al*: βII-Spectrin (SPTBN1) suppresses progression of hepatocellular carcinoma and Wnt signaling by regulation of Wnt inhibitor kallistatin. Hepatology 61: 598-612, 2015.
9. Li R, Xu J, Wong DS, Li J, Zhao P and Bian L: Self-assembled N-cadherin mimetic peptide hydrogels promote the chondrogenesis of mesenchymal stem cells through inhibition of canonical Wnt/β-catenin signaling. Biomaterials 145: 33-43, 2017.
10. Yang S, Liu Y, Li MY, Ng CS, Yang SL, Wang S, Zou C, Dong Y, Du J, Long X, *et al*: FOXP3 promotes tumor growth and metastasis by activating Wnt/β-catenin signaling pathway and EMT in non-small cell lung cancer. Mol Cancer 16: 124, 2017.
11. Wei CY, Zhu MX, Yang YW, Zhang PF, Yang X, Peng R, Gao C, Lu JC, Wang L, Deng XY, *et al*: Downregulation of RNF128 activates Wnt/β-catenin signaling to induce cellular EMT and stemness via CD44 and CTTN ubiquitination in melanoma. J Hematol Oncol 12: 21, 2019.
12. Chen L, Li M, Li Q, Wang CJ and Xie SQ: DKK1 promotes hepatocellular carcinoma cell migration and invasion through β-catenin/MMP7 signaling pathway. Mol Cancer 12: 157, 2013.
13. Villar J, Cabrera NE, Casula M, Valladares F, Flores C, López-Aguilar J, Blanch L, Zhang H, Kacmarek RM and Slutsky AS: WNT/β-catenin signaling is modulated by mechanical ventilation in an experimental model of acute lung injury. Intensive Care Med 37: 1201-1209, 2011.
14. Russell JO and Monga SP: Wnt/β-catenin signaling in liver development, homeostasis, and pathobiology. Annual Rev Pathol 13: 351-378, 2018.
15. Zhang R, Lin HM, Broering R, Shi XD, Yu XH, Xu LB, Wu WR and Liu C: Dickkopf-1 contributes to hepatocellular carcinoma tumorigenesis by activating the Wnt/β-catenin signaling pathway. Signal Transduct Target Ther 4: 54, 2019.
16. Chen J, Rajasekaran M, Xia H, Zhang X, Kong SN, Sekar K, Seshachalam VP, Deivasigamani A, Goh BK, Ooi LL, *et al:* The microtubule-associated protein PRC1 promotes early recurrence of hepatocellular carcinoma in association with the Wnt/β-catenin signalling pathway. Gut 65: 1522-1534, 2016.
17. Zuo Q, He J, Zhang S, Wang H, Jin G, Jin H, Cheng Z, Tao X, Yu C, Li B, *et al*: PPARγ Coactivator-1α suppresses metastasis of hepatocellular carcinoma by inhibiting warburg effect by PPARγ-dependent WNT/β-catenin/Pyruvate dehydrogenase kinase isozyme 1 axis. Hepatology 73: 644-660, 2021.
18. Wardhani LO, Matsushita M, Iwasaki T, Kuwamoto S, Nonaka D, Nagata K, Kato M, Kitamura Y and Hayashi K: Expression of the IDO1/TDO2-AhR pathway in tumor cells or the tumor microenvironment is associated with merkel cell polyomavirus status and prognosis in merkel cell carcinoma. Hum Pathol 84: 52-61, 2019.
19. Cheong JE and Sun L: Targeting the IDO1/TDO2-KYN-AhR pathway for cancer immunotherapy-challenges and opportunities. Trends Pharmacol Sci 39: 307-325, 2018.
20. Chung DJ, Rossi M, Romano E, Ghith J, Yuan J, Munn DH and Young JW: Indoleamine 2,3-dioxygenase-expressing mature human monocyte-derived dendritic cells expand potent autologous regulatory T cells. Blood 114: 555-563, 2009.
21. Fallarino F, Grohmann U, You S, McGrath BC, Cavener DR, Vacca C, Orabona C, Bianchi R, Belladonna ML, Volpi C, *et al*: The combined effects of tryptophan starvation and tryptophan catabolites down-regulate T cell receptor zeta-chain and induce a regulatory phenotype in naive T cells. J Immunol 176: 6752-6761, 2006.
22. Li S, Zhang W, Wu C, Gao H, Yu J, Wang X, Li B, Jun Z, Zhang W, Zhou P, *et al*: HOXC10 promotes proliferation and invasion and induces immunosuppressive gene expression in glioma. FEBS J 285: 2278-2291, 2018.
23. Li S, Weng J, Song F, Li L, Xiao C, Yang W and Xu J: Circular RNA circZNF566 promotes hepatocellular carcinoma progression by sponging miR-4738-3p and regulating TDO2 expression. Cell Death Dis 11: 452, 2020.
24. Muller AJ, Manfredi MG, Zakharia Y and Prendergast GC: Inhibiting IDO pathways to treat cancer: Lessons from the ECHO-301 trial and beyond. Semin Immunopathol 41: 41-48, 2019.
25. Lee SH, Mahendran R, Tham SM, Thamboo TP, Chionh BJ, Lim YX, Tsang WC, Wu QH, Chia JY, Tay MHW, *et al:* Tryptophan-kynurenine ratio as a biomarker of bladder cancer. BJU Int 127: 445-453, 2021.
26. Livak KJ and Schmittgen TD: Analysis of relative gene expression data using real-time quantitative PCR and the 2(-Delta Delta C(T)) method. Methods 25: 402-408, 2001.
27. Schmitt M, Metzger M, Gradl D, Davidson G and Orian-Rousseau V: CD44 functions in Wnt signaling by regulating LRP6 localization and activation. Cell Death Differ 22: 677-689, 2015.
28. Lv YF, Dai H, Yan GN, Meng G, Zhang X and Guo QN: Downregulation of tumor suppressing STF cDNA 3 promotes epithelial-mesenchymal transition and tumor metastasis of osteosarcoma by the Wnt/GSK-3β/β-catenin/Snail signaling pathway. Cancer Lett 373: 164-173, 2016.
29. D'Amato NC, Rogers TJ, Gordon MA, Greene LI, Cochrane DR, Spoelstra NS, Nemkov TG, D'Alessandro A, Hansen KC and Richer JK: A TDO2-AhR signaling axis facilitates anoikis resistance and metastasis in triple-negative breast cancer. Cancer Res 75: 4651-4664, 2015.
30. Creelan BC, Antonia S, Bepler G, Garrett TJ, Simon GR and Soliman HH: Indoleamine 2,3-dioxygenase activity and clinical outcome following induction chemotherapy and concurrent chemoradiation in Stage III non-small cell lung cancer. Oncoimmunology 2: e23428, 2013.
31. Yang H, Fang F, Chang R and Yang L: MicroRNA-140-5p suppresses tumor growth and metastasis by targeting transforming growth factor β receptor 1 and fibroblast growth factor 9 in hepatocellular carcinoma. Hepatology 58: 205-217, 2013.
32. Wu D, Zhang J, Lu Y, Bo S, Li L, Wang L, Zhang Q and Mao J: miR-140-5p inhibits the proliferation and enhances the efficacy of doxorubicin to breast cancer stem cells by targeting Wnt1. Cancer gene therapy 26: 74-82, 2019.
33. Fu J, Cai H, Wu Y, Fang S and Wang D: Elevation of FGD5-AS1 contributes to cell progression by improving cisplatin resistance against non-small cell lung cancer cells through regulating miR-140-5p/WEE1 axis. Gene 755: 144886, 2020.
34. Lan H, Chen W, He G and Yang S: miR-140-5p inhibits ovarian cancer growth partially by repression of PDGFRA. Biomed Pharmacother 75: 117-122, 2015.
35. Guastella AR, Michelhaugh SK, Klinger NV, Fadel HA, Kiousis S, Ali-Fehmi R, Kupsky WJ, Juhász C and Mittal S: Investigation of the aryl hydrocarbon receptor and the intrinsic tumoral component of the kynurenine pathway of tryptophan metabolism in primary brain tumors. J Neuro Oncol 139: 239-249, 2018.
36. Mohapatra SR, Sadik A, Tykocinski LO, Dietze J, Poschet G, Heiland I and Opitz CA: Hypoxia inducible factor 1α inhibits the expression of immunosuppressive tryptophan-2,3-dioxygenase in glioblastoma. Front Immunol 10: 2762, 2019.
37. Greene LI, Bruno TC, Christenson JL, D'Alessandro A, Culp-Hill R, Torkko K, Borges VF, Slansky JE and Richer JK: A role for tryptophan-2,3-dioxygenase in CD8 T-cell suppression and evidence of tryptophan catabolism in breast cancer patient plasma. Mol Cancer Res 17: 131-139, 2019.
38. Azuma A, Kudoh S, Nakashima M and Nagatake T: A double-blind study of zaltoprofen for the treatment of upper respiratory tract infection. Pharmacology 85: 41-47, 2010.
39. Ohyama T, Sato K, Kishimoto K, Yamazaki Y, Horiguchi N, Ichikawa T, Kakizaki S, Takagi H, Izumi T and Mori M: Azelnidipine is a calcium blocker that attenuates liver fibrosis and may increase antioxidant defence. Br J Pharmacol 165: 1173-1187, 2012.